ley, Phys. Rev. C 1, 1455 (1970).
[10]P. D. Kuntz, University of Colorado Report No. COO-535-606, 1969 (unpublished).
[11]W. R. Hering, H. Becker, C. A. Wiedner, and W. J. Thompson, Nucl. Phys. A151, 33 (1970); W. J. Thompson and W. R. Hering, Phys. Rev. Letters 24, 272 (1970).
[12]R. W. Zurmühle and C. M. Fou, Nucl. Phys. A129, 502 (1969).
[13]G. Th. Kaschl, G. Mairle, U. Schmidt-Rohr, and G. J. Wagner, Nucl. Phys. A136, 286 (1969).
[14]B. H. Wildenthal, J. B. McGrory, E. C. Halbert, and H. D. Graber, Phys. Rev. C 4, 1708 (1971).
[15]R. Huby, in *Progress in Nuclear Physics*, edited by O. R. Frisch (Butterworths, London, 1953).
[16]H. Kattenborn, C. Mayer-Böricke, and B. Mertens, Nucl. Phys. A119, 559 (1968).
[17]R. Mohan, M. Danos, and L. C. Biedenharn, Phys. Rev. C 3, 468 (1971).
[18]G. F. Bertsch, Nucl. Phys. A142, 499 (1970).
[19]H. C. Lee and R. Y. Cusson, to be published.

PHYSICAL REVIEW C VOLUME 5, NUMBER 4 APRIL 1972

Reaction ^{27}Al$(d, p)^{28}$Al at $E_d = 23$ MeV*

J. V. Maher,† H. T. Fortune,‡ G. C. Morrison, and B. Zeidman
Argonne National Laboratory, Argonne, Illinois 60439

(Received 15 November 1971)

The reaction ^{27}Al$(d, p)^{28}$Al has been investigated at a deuteron energy of 23 MeV. Distorted-wave analyses of the angular distributions for the low-lying states of ^{28}Al have been carried out for several sets of optical-model parameters. The spectroscopic factors obtained for states up to 2.66-MeV excitation in ^{28}Al are in qualitative agreement with shell-model predictions. It is found, however, that the results of analysis are sensitive to the choice of parameters, and there is difficulty in extracting reliable quantitative spectroscopic information from this reaction without the use of information from other reactions.

I. INTRODUCTION

Until recently the nucleus ^{28}Al has not been extensively studied. Early experiments established its level scheme[1,2] and assigned spins and parities[3] for several of the low-lying levels. But prior to a preliminary publication[4] of this 23-MeV ^{27}Al(d, p) work, ^{28}Al had not been populated by a nucleon-transfer reaction at a bombarding energy at which such a reaction could be expected to be dominated by direct processes. A previous ^{27}Al(d, p) experiment[2] at $E_d = 7$ MeV established l_n values for most states, but extracted spectroscopic strengths with the plane-wave Born approximation.

Further understanding of the spectroscopy of ^{28}Al is of interest for several reasons. The prolate deformations typical of nuclei in the mass region $20 \leq A \leq 24$ decrease with increasing mass, and nuclei in the region $A = 27, 28$ are believed[5,6] to be either spherical or only slightly deformed. There is some evidence of oblate deformation[7] at still larger mass, so that the $A \approx 28$ nuclei provide an interesting testing ground for extended shell-model and Nilsson-model calculations. Although ^{28}Al is an odd-odd nucleus, its level scheme is very simple[8] up to $E_x \approx 3$ MeV. (There are 12 states in this region of excitation.)

In the simple shell model, the $^{28}_{13}\mathrm{Al}_{15}$ ground state would be a $[\pi(1d_{5/2})^{-1}\nu(2s_{1/2})]_{2^+,3^+}$ doublet. Four states from the configuration

$$[\pi(1d_{5/2})^{-1}\nu(1d_{3/2})]_{1^+,2^+,3^+,4^+}$$

would also be expected at low excitation energies. Obviously, such a picture is too simple, but the shell-model calculation in the accompanying paper[9] has been quite successful in predicting excitation energies and further properties of the first 12 levels of ^{28}Al. Nilsson-model calculations have also been performed[10] for ^{28}Al, but these have not been extended beyond the first six levels.

The recent interest in the spectroscopy of the mid-$2s1d$ shell has prompted several experiments for the study of ^{28}Al. Quite a complete experimental picture is now available for this nucleus. Spectroscopic factors (present work), branching ratios,[11,12] lifetimes,[9] and spin assignments[8,11,12] are now available and all agree rather well with shell-model predictions, as will be discussed later.

A further feature in this study has been a comparison of distorted-wave Born-approximation (DWBA) predictions for ^{27}Al$(d, p)^{28}$Al by use of several sets of deuteron and proton optical potentials. Such an investigation was thought to be

worthwhile, since consistent sets of parameters do not yet exist for this region.

Section II discusses the details of data acquisition, and Sec. III presents the data. Section IV discusses the distorted-wave calculations which were performed. Section V considers the spectroscopy of ^{28}Al, and Sec. VI summarizes the results of this study.

II. EXPERIMENTAL ARRANGEMENT

^{27}Al$(d, p)^{28}$Al angular distributions were measured in two separate experiments. In each experiment, a self-supporting Al target (~100 μg/cm^2 thick) was bombarded with 23-MeV deuterons from the Argonne cyclotron. Angular distributions of outgoing protons were measured in an 18-in. scattering chamber for laboratory scattering angles between 9 and 30°. In this case a telescope of four Au-Si surface-barrier detectors was used to determine the energies and identify the species of the reaction products. The first two thin detectors were used as a standard telescope for ^{3}He and tritons and were summed to give a first signal for protons and deuterons. Signals from the last two detectors (each 2000 μm thick) were summed to complete the proton-deuteron telescope. Mass and charge analysis of the telescope pulses was performed in two analog multipliers, and the output pulses from the multipliers were used to route spectra into four 1024-channel quadrants of a Packard analyzer. The energy resolution width was typically ~50 keV for all reactions studied. The total dead time of the system and a first-order correction to the dead-time measurement were monitored by a system described previously.[13] Thus stripping (and pickup) cross sections were known very accurately relative to elastic scattering cross sections. The pickup reactions are discussed separately[14] and the remainder of this paper will discuss only the (d, p) reaction, but it is of interest to note that the absolute normalization of the (d, p) data is constrained by considerations discussed in detail in Ref. 14. Briefly, the absolute cross sections were determined by normalizing the elastic scattering data to the optical potential used in Ref. 14. This normalization agrees within expected errors with target-thickness estimates and sum-rule considerations applied to the pickup reactions.

In the second experiment, an Enge split-pole spectrograph was used to measure ^{27}Al(d, p) reaction cross sections at laboratory angles of 5, 7, and 9°. Emulsions placed in the focal plane of the spectrograph were used to detect outgoing protons and were later scanned automatically.[15] Resolution was ~12 keV.

III. DATA PRESENTATION

Spectra for the ^{27}Al(d, p) reaction are shown in Fig. 1 (12° spectrum taken with the Au-Si detector telescope) and Fig. 2 (5° spectrum measured in the split-pole spectrograph). The program AUTOFIT[16] allowed the extraction of peak areas even for closely spaced peaks such as those of

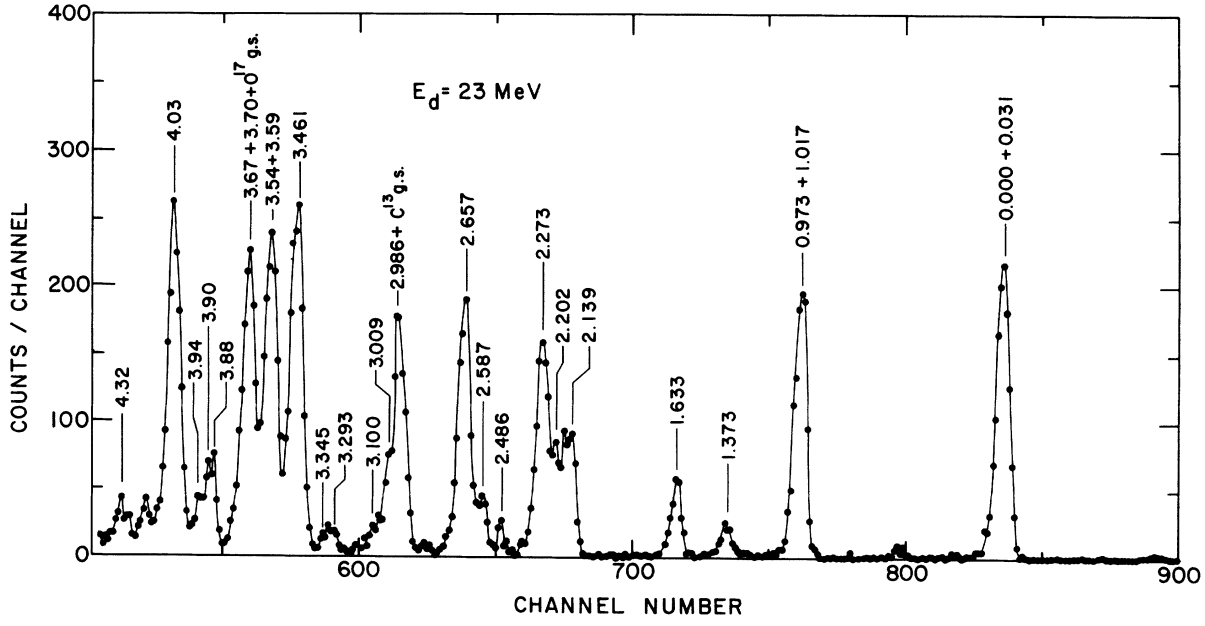

FIG. 1. ^{27}Al$(d, p)^{28}$Al spectrum obtained with a counter telescope at $\theta_{lab} = 12°$.

the triplet 2.14, 2.21, and 2.28 MeV. The spectrograph data resolved even more closely spaced states, such as the ground-state doublet. Angular distributions for ^{28}Al states populated in the $^{27}Al(d,p)$ reaction are shown in Figs. 3 and 4. For several of the states that were seen and identified, it was not possible to extract meaningful angular distributions – either because the state was very weakly populated at most angles or because the oxygen or carbon impurity peaks seen in Fig. 1 obscured the state at most angles. Table I lists the excitation energy for each of these states and the cross section at an angle at which it can be reliably determined.

Some of the angular distributions in Figs. 3 and 4 lack data points at the two most forward angles. Since the spectrograph data were measured to allow improved determination of $l=0$ spectroscopic factors and since the $l=0$ angular distributions increase sharply as the angle decreases toward 0°, it was necessary to sacrifice counting statistics for weak states of higher l value in order to avoid overexposing the plates for the $l=0$ states. Finally, some states reported in low-energy (d,p) studies[1,2] were not seen at all. A notable example is the state at 0.973 MeV, which must be populated entirely through multistep processes at low bombarding energies.

IV. DISTORTED-WAVE ANALYSIS

A. Calculations with Several Potential Sets

The literature exhibits many discrepancies between the spectroscopic factors extracted in different direct-reaction studies in the mid-2s1d shell. It is of interest to determine whether these discrepancies arise from poor data acquisition, poor data analysis, inadequacies in the distorted-wave treatment, or some combination of all these factors. For this reason, distorted-wave calculations were performed for several sets of optical potentials that have been used in this or neighbor-

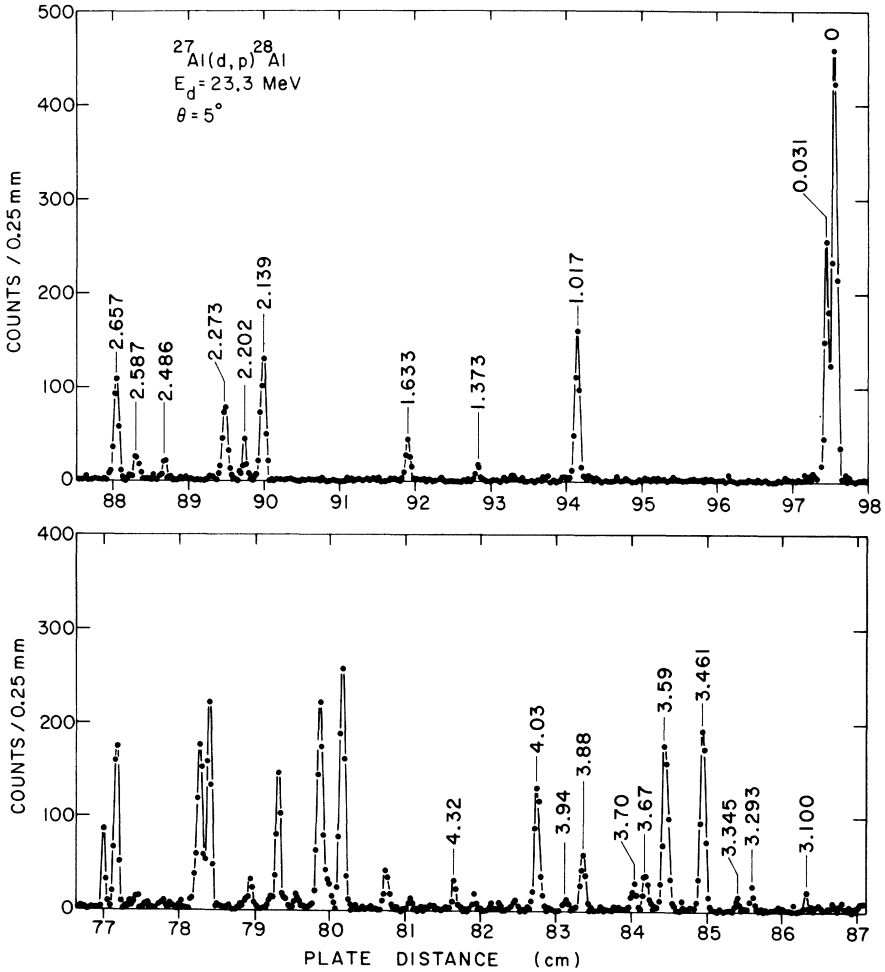

FIG. 2. $^{27}Al(d,p)^{28}Al$ spectrum obtained with a split-pole spectrograph at $\theta_{lab} = 5°$.

TABLE I. Weak states (and states obscured at several angles by impurities) seen in the ^{27}Al(d,p) reaction at 23 MeV.

E_x (MeV)	l (Ref. 2)	$d\sigma/d\omega$ ($\theta_{c.m.}$) (mb/sr)	Approximate [a] $(2J+1)S$
2.99, 3.01	2	0.07 (25°)	0.63
3.10	2	0.3 (9.4°)	0.89
3.29	0	0.3 (12.6°)	0.45
3.35	0	0.07 (19°)	0.55
3.67	0	0.24 (25°)	0.78
3.70	0		
3.88	1		
3.90		0.91 (12.6°)	...
3.94	0+2		

[a] Based on only one angle.

ing mass regions, and the results were compared for adequacy of fit and – given adequate fit to the shape of angular distributions – for consistency of spectroscopic information.

Parameters specifying the potentials that were considered are listed in Table II. The first of the deuteron potentials[17] (D1) fits the ^{26}Mg$+d$ elastic scattering data at $E_d = 21$ MeV and has a small real radius, a strong real spin-orbit potential, and a strong surface-imaginary potential. Potential D2,[18] the only volume-absorption potential considered, is the only deuteron potential we have found[14] to fit $l=2$ (d,t) and $(d,{}^3\mathrm{He})$ transitions in the mass region $25 \leq A \leq 27$. This potential, which is characterized by a large radius for both the real and the imaginary wells and the absence of spin-orbit coupling, is the one used to normalize the ^{27}Al$+d$ elastic scattering angular distribution. The elastic scattering angular distribution predicted by this potential is shown along with the measured elastic scattering data in Fig. 5. Elastic scattering cross sections calculated with all of the other deuteron potentials considered agree with this data normalization to within 20%. Although D2 is not a "best-fit" potential, it can be seen to reproduce the shape of the elastic scattering angular distribution.

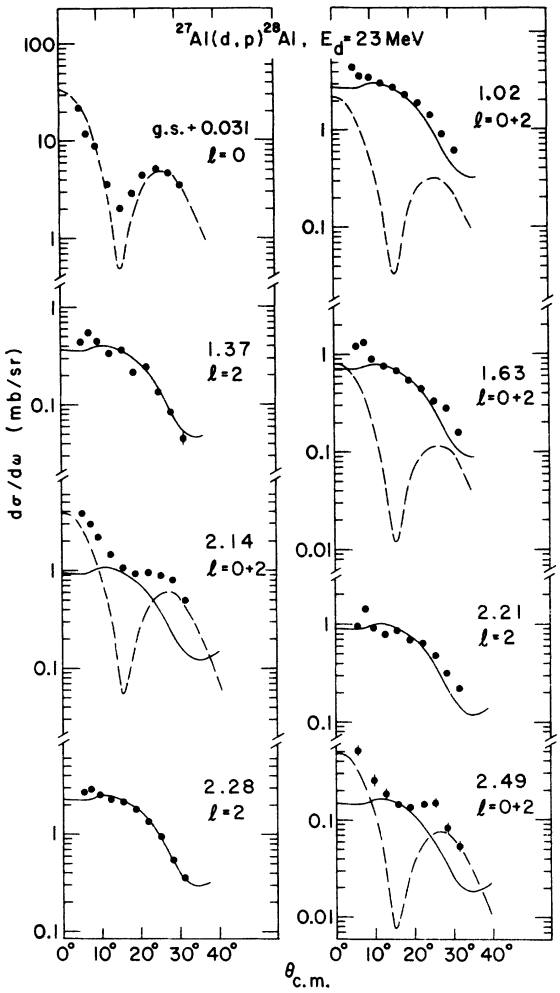

FIG. 3. Angular distributions for ^{28}Al states populated by the ^{27}Al(d,p) reaction at $E_d = 23$ MeV. Curves are DWBA fits to the data as discussed in the text.

Both the D3 potential[19] and the D4 potential[6] resulted from fits to deuteron elastic scattering data in the mid-2s1d shell. D3 uses spin-orbit coupling while D4 does not, and both have surface-derivative imaginary potentials.

P1 is Perey's proton potential.[20] It arose from fitting $p+{}^{27}$Al data at energies below 22 MeV. P2

TABLE II. Optical potentials used in DWBA analysis of ^{27}Al$(d,p)^{28}$Al data at $E_d = 23$ MeV.

Potential	System	V (MeV)	W (MeV)	$r_0 = r_{so}$ (fm)	r_{0C} (fm)	$a = a_{so}$ (fm)	V_{so} (MeV)	W_D (MeV)	r'_0 (fm)	a' (fm)
D1	^{27}Al$+d$	100	0	0.969	1.00	0.853	9	24.107	1.33	0.651
D2	^{27}Al$+d$	100	16.5	1.40	1.40	0.60	0	0	1.74	0.80
D3	^{27}Al$+d$	105	0	1.02	1.30	0.86	6	20	1.42	0.65
D4	^{27}Al$+d$	123	0	0.89	1.30	0.945	0	27.3	1.385	0.539
P1	^{28}Al$+p$	43.5	0	1.25	1.25	0.65	8.5	9.02	1.25	0.47
P2	^{28}Al$+p$	55	0	1.124	1.124	0.57	5.5	8	1.124	0.50
P3	^{28}Al$+p$	50.4	5.49	1.108	1.108	0.705	5.92	2.03	1.407	0.521

is an extrapolation of the potential of Watson, Singh, and Segel,[21] which fitted data throughout the $1p$ shell. Satchler[22] reports that P3 fits $p+^{28}$Si scattering at 40 MeV. All three proton potentials include real spin-orbit terms and surface-derivative imaginary terms. P3 also has a volume imaginary part.

All deuteron potentials considered have real well depths of ~100 MeV and all three proton potentials have real well depths of ~50 MeV. Preliminary calculations indicated that for the angular range of interest in this study, finite-range nonlocal calculations yielded the same shape of the angular distribution and the same Q dependence as zero-range local (ZRL) calculations. Differences between these two calculated values of the absolute cross sections were typically about 25%. Thus all but the final calculations reported herein were performed in the ZRL approximation. ZRL calculations for several values of l transfer and Q were carried out with various combinations of the potentials listed in Table II. The code JULIE[23] was used to perform these calculations.

Potential D1 was the only one that could easily be excluded on the basis of the shapes of its predicted angular distributions. This feature is illustrated in Figs. 6 and 7, where the data are compared with predictions of each of the four deuteron potentials in combination with P2. Figure 6 shows the best fit of each of the four predicted angular distributions to the strong pure $l=0$ ground-state transition, while Fig. 7 shows best fits of each of the potential combinations to the strong pure $l=2$ transition that populates the 2.28-MeV state in ^{28}Al. As can be seen from Figs. 6 and 7, the combinations of deuteron potentials D2, D3, and D4 with proton potential P2 all give acceptable fits to the $l=2$ angular distribution. There is a slight preference for D2, since it fits the large-angle falloff best, while the seriousness of its slight failure at small angles is mitigated by the large possible error in normalizing the two forward spectrograph points. Similarly, all three deuteron potentials yield acceptable predictions for the positions of the first minimum and second maximum of the $l=0$ angular distribution, although D4 misses the first minimum by ~$2\frac{1}{2}°$ and D3 places the first minimum too far forward by ~2°. None of the three give a good account of the relative

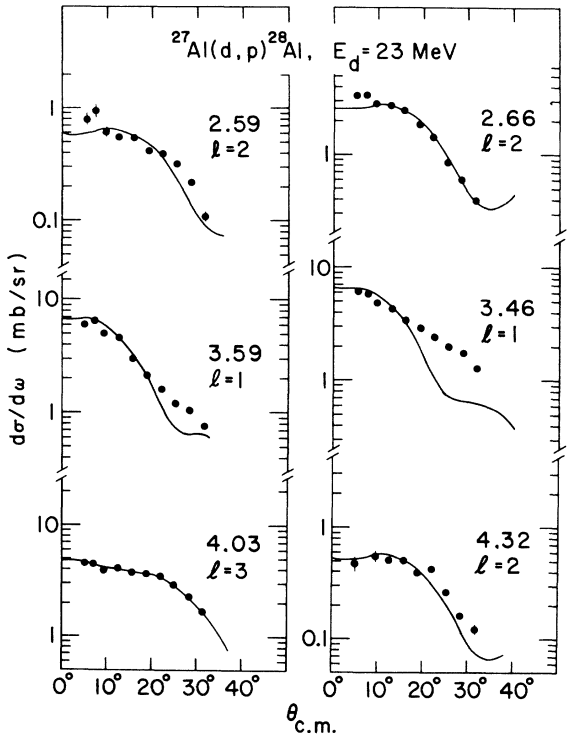

FIG. 4. Angular distributions for ^{28}Al states populated by the ^{27}Al(d,p) reaction at $E_d=23$ MeV. Curves are DWBA fits to the data as discussed in the text.

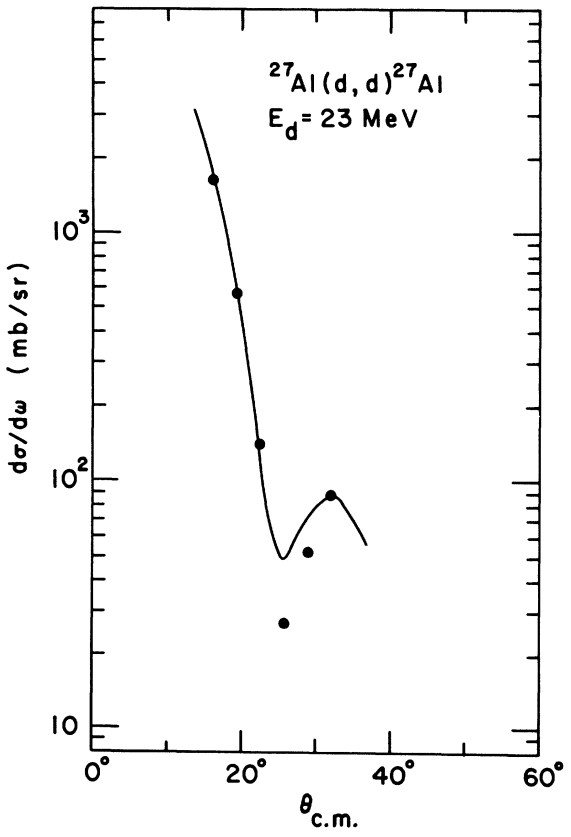

FIG. 5. Angular distributions for elastic scattering of 23-MeV deuterons from ^{27}Al. The curve represents the prediction of the optical potential D2 (Table II). Data have been normalized to fit this curve.

heights of the first and second maxima. The $l=0$ fits also show a slight preference for D2, and this is enhanced by the success of D2 (and the corresponding failure of D3 and D4) in fitting the $l=2$ (d,t) and $(d,{}^3\mathrm{He})$ angular distributions over a wide range of Q values in this mass region.[14] For these reasons, the final finite-range nonlocal (FRNL) calculations were performed with D2. However, it must be emphasized that the two other potentials give almost equally good accounts of the data; the systematics of their spectroscopic predictions relative to those of D2 will be discussed below.

Predictions of D2 with P1, P2, and P3 for the same two strong states are shown in Fig. 8 (for $l=0$) and Fig. 9 (for $l=2$). All do well for the $l=2$ transition. P1 is clearly preferable for $l=0$, since it fits both maxima. Not only is this improvement in $l=0$ fit important enough to justify using P1 for the final calculations discussed below, but it is also especially crucial for a reaction on a target with nonzero spin, e.g., for the $^{27}\mathrm{Al}(d,p)$ reaction. For this reaction, the good fit to both maxima in pure $l=0$ transitions lends confidence to values extracted for $l=0$ admixtures in mixed-l transitions discussed below.

Spectroscopic strengths $(2J+1)S$ have been extracted for the strong $l=0$ and $l=2$ transitions used above in Figs. 6–9. These are listed in Table III for each of the potential combinations discussed above. Also shown for each potential combination and each state is $(2J+1)S$ for a fictitious state of identical cross section (and angular-distribution shape) but with a Q value 2 MeV more negative than that for the original state. Not only can it be seen that the absolute spectroscopic strength varies from one potential to another, but also there is a variation in l dependence and Q dependence which makes the spectroscopic factors reported in the next section less reliable than they are normally thought to be.

B. Spectroscopic Factors

Using the potential pair D2-P1 discussed above, FRNL calculations with the code DWUCK[24] were performed for $^{28}\mathrm{Al}$ states populated in the $^{27}\mathrm{Al}(d,p)$ reaction. The bound-state well parameters are $r_0=1.25$ fm, $a=0.65$ fm, and $\lambda=25$. The (d,p) finite-range parameter is 0.62 fm, while the nonlocality parameters are $\beta_d=0.54$ fm, $\beta_p=0.85$ fm, and $\beta_n=0$. The solid curves shown in Figs. 3 and 4 result from fitting the calculated FRNL angular distributions to the experimental angular distribu-

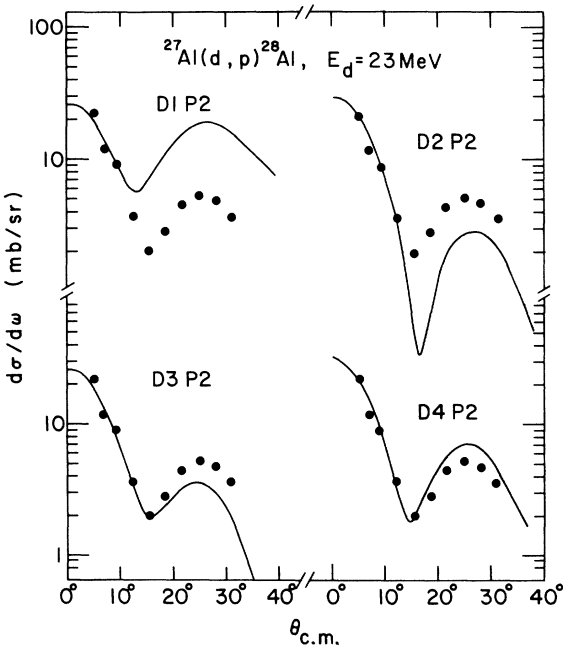

FIG. 6. Best fits of distorted-wave calculations to the $l=0$ angular distribution of the $^{28}\mathrm{Al}$ ground-state doublet. Predictions for each of the deuteron potentials D1, D2, D3, and D4 in conjunction with the proton potential P2 are shown as curves normalized to the experimental angular distributions.

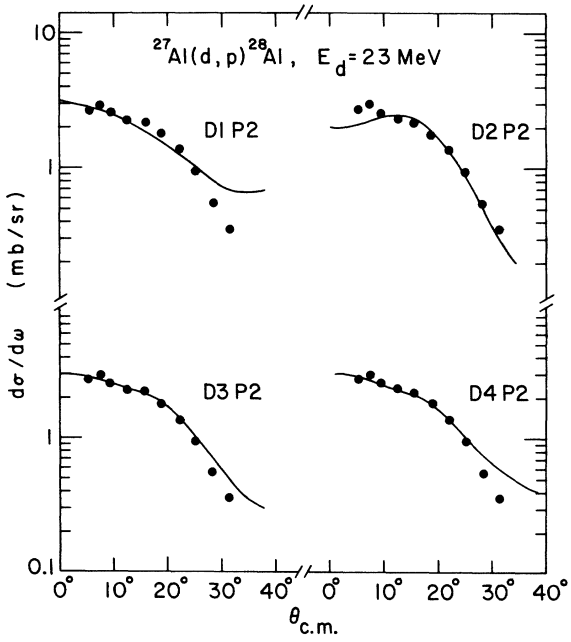

FIG. 7. Best fits of distorted-wave calculations to the $l=2$ angular distribution for the 2.28-MeV state of $^{28}\mathrm{Al}$. Predictions for each of the deuteron potentials D1, D2, D3, and D4 in conjunction with the proton potential P2 are shown as curves normalized to the experimental angular distributions.

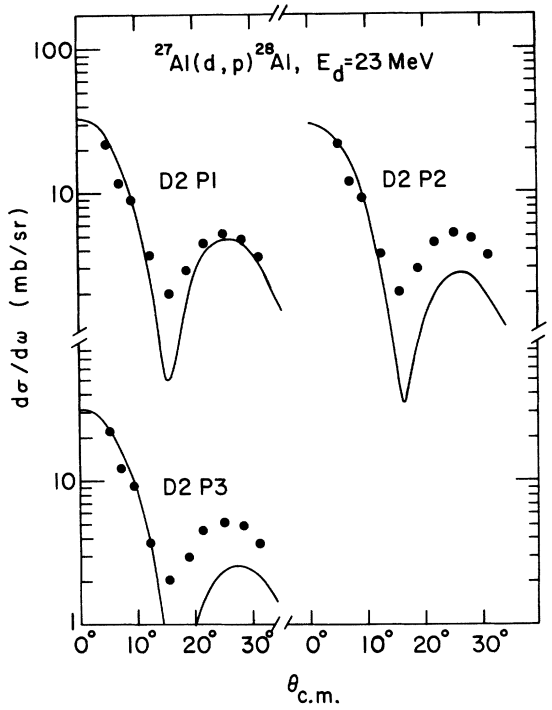

FIG. 8. Best fits of distorted-wave calculations to the $l = 0$ angular distribution for the 2.28-MeV state of ^{28}Al. Predictions for each of the proton potentials P1, P2, and P3 in conjunction with the deuteron potential D2 are shown as curves normalized to the experimental angular distributions.

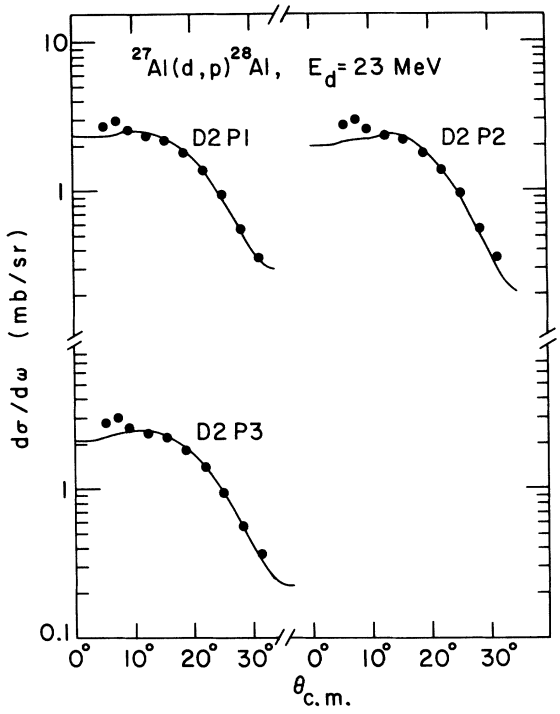

FIG. 9. Best fits of distorted-wave calculations to the $l = 2$ angular distribution for the 2.28-MeV state of ^{28}Al. Predictions for each of the proton potentials P1, P2, P3 in conjunction with the deuteron potential D2 are shown as curves normalized to the experimental angular distributions.

tions shown in the figures. Spectroscopic factors have been extracted by use of the relation

$$\sigma_{\text{exp}}(\theta) = \frac{N(2J_f+1)}{2J_i+1} \sum_{lj} \frac{S_{lj}\sigma_{lj}^{\text{DW}}(\theta)}{2j+1} .$$

For the (d, p) reaction, $N = 1.53$. J_i is the spin of the target ground state (which for ^{27}Al is $\frac{5}{2}$), and J_f is the spin of the final state of the residual nucleus. Table IV lists excitation energies E_x, l values, and the products $(2J_f+1)S_l$ for the states populated in this study. All $l = 2$ spectroscopic strengths shown were obtained on the assumption of $d_{3/2}$ transfer. If the j transfer is $\frac{5}{2}$, the value of S should be decreased by about 30%. In addition to the ~25% limitation inherent in spectroscopic-factor determinations with the DWBA, all the difficulties discussed above decrease the reliability of the spectroscopic factors listed in Table IV.

This decrease in reliability of the distorted-wave analysis may, as discussed above, account for many of the discrepancies between various direct-reaction experiments performed in this mass region. Also, the spectroscopic strengths for the weak and partially obscured states listed

TABLE III. Values of $(2J_{fl}+1)S_l$ for the $l = 0$ transition to the ground-state doublet and the $l = 2$ transition to the 2.28-MeV state as calculated with several sets of optical potentials – all of which give good fits to the experimental angular distributions. For convenience in this table, the value of $(2J_{fl}+1)S_l$ for the ground-state doublet is normalized to 1 for potential set D2-P1.

Potential set	$(2J_{f0}+1)S_0$ g.s. doublet	$(2J_{f2}+1)S_2$ 2.28-MeV state	$\frac{(2J_{f0}+1)S_0}{(2J_{f2}+1)S_2}$	$(2J_{f0}+1)S_0$ $Q_0 - 2$ MeV	$(2J_{f2}+1)S_2$ $Q_2 - 2$ MeV	$\frac{(2J_{f0}+1)S_0}{(2J_{f2}+1)S_2}$ $Q - 2$ MeV
D2-P1	1.0	0.56	1.8	0.84	0.40	2.1
D2-P2	0.80	0.49	1.7	0.80	0.37	2.2
D2-P3	0.75	0.33	2.3	0.72	0.35	2.1
D3-P2	0.51	0.13	3.9	0.54	0.13	4.2
D4-P2	0.58	0.17	3.4	0.64	0.17	3.8

in Table I were roughly determined for use in Sec. V. These estimates, shown in column 3 of Table I, were based on the l-value determination of Buechner, Mazari, and Sperduto.[1]

V. DISCUSSION

Of the 12 states up to 2.66-MeV excitation in ^{28}Al, only the 0.973-MeV state was not populated in this experiment. Since the ground-state doublet is populated by virtually pure $l=0$ transfer, it is possible to use the forward-angle spectrograph exposures to apportion the spectroscopic strength unambiguously between the members of the ground-state doublet. These strengths are listed in Table V, where they are compared with the shell-model predictions from the accompanying paper.[9] (In this table, the ground-state strength has been renormalized to the shell-model value.) The relative $l=0$ strengths of the two members of the ground-state doublet are well accounted for by the shell-model calculation.

An $l=2$ strength of the magnitude the shell model predicts for the ground-state doublet would correspond to a maximum $l=2$ contribution of 0.4 mb/sr to the cross section. This small amount of $l=2$ may be present in the data, but could not be detected in the presence of the large $l=0$ strength seen for these states. Thus, the lack of experimentally observable $l=2$ strength does not argue against the shell-model ground-state wave function.

The model calculation is qualitatively in agreement with the experimental result for the next three excited states (0.973, 1.017, and 1.372 MeV). The first serious discrepancies arise for the states at 1.633 and 2.14 MeV. (Note that the state here labeled 1.633 MeV is known[9,12] to be a doublet and that the shell model predicts pure $l=2$ for one member of the doublet and mixed $l=0$, $l=2$ strength for the other.) In each of these cases, the $l=0$ strength seen experimentally is greater than the shell model predicts. It is difficult to assess the seriousness of this discrepancy, since (a) the experimental number is a small fraction of the total $l=0$ strength; (b) the data points that force this $l=0$ strength up to its listed value result from normalizing spectrograph data to counter data and thus, as discussed above, must entail errors somewhat larger than the statistical errors shown in the data; and (c) the relative strengths for states populated by mixed l values have an additional uncertainty because pure l transitions are not fitted perfectly by the calculations.

The results for the remainder of the states up to 2.66 MeV in Table V are basically in agreement with theory – with the exception of the state at 2.21 MeV. This $l=2$ transition is strong, and no good reason for the failure of the model for this state presents itself.

Thus the qualitative agreement between shell-model and experimental results is satisfactory for $l=0$ and $l=2$ strengths – i.e., states predicted to be strong are strong and states observed to be

TABLE IV. ^{27}Al$(d,p)^{28}$Al spectroscopic factors.

E_x (MeV)	J^π	nl_j	$(2J_f+1)S$
0.000	3^+	$2s_{1/2}$	9.7
0.031	2^+	$2s_{1/2}$	5.4
1.017	3^+	$2s_{1/2}$	0.97
		$1d_{3/2}$	14.1
1.372	1^+	$1d_{3/2}$	1.76
1.633	$1^+, 2^+$	$2s_{1/2}$	0.35
		$1d_{3/2}$	3.2
2.14	3^+	$2s_{1/2}$	1.7
		$1d_{3/2}$	4.0
2.21	1^+	$1d_{3/2}$	3.7
2.28	$(2, 3, 4)^+$	$1d_{3/2}$	9.2
2.49	2^+	$2s_{1/2}$	0.21
		$1d_{3/2}$	0.58
2.59	$(5)^+$	$1d_{3/2}$	2.3
2.66	$(4)^+$	$1d_{3/2}$	9.7
3.46	4^-	$2p_{3/2}$	4.3
3.54 +3.59	$(2-4)^-$	$2p_{3/2}$	4.3
4.03	$(0-6)^-$	$1f_{7/2}$	16
4.32	$(0-5)^+$	$1d_{3/2}$	1.3

TABLE V. Values of $(2J+1)S$ for the reaction ^{27}Al$(d,p)^{28}$Al.

E_x (MeV)	$l=0$ transitions Exp.	Theory	$l=2$ transitions Exp.	Theory	Odd-l transitions
0.000	4.6 [a]	4.6 [a]	b	0.68	
0.031	2.6	2.8	b	0.53	
0.973	~0	···	~0	0.15	
1.017	0.46	0.12	6.7	2.4	
1.372	···	···	0.83	0.18	
1.633	0.16	0.03	1.5	0.51	
2.14	0.78	0.07	1.9	1.55	
2.21	···	···	1.7	0.04	
2.28	···	···	4.4	0.64	
2.49	0.10	0.00	0.28	0.02	
2.59	···	···	1.1	0.49	
2.66	···	···	4.6	3.4	
3.46					$l=1$: 2.0
3.54 +3.59					$l=1$: 2.0
4.03					$l=3$: 7.4
4.32			0.63		

[a] The experimental value was normalized to the theoretical one by dividing S_{exp} by 2.1.
[b] See discussion in text.

weak are indeed predicted to be weak. However, the $l = 2$ experimental strengths are systematically stronger than the calculated strengths because the shell-model calculation predicts that most of the $1d$ strength is spread over many weak states at higher excitation energies. The arbitrary experimental normalization discussed above is attractive in that it not only allows state-to-state comparison with the shell-model predictions, but also puts 88% of the $l = 0$ and $l = 2$ sum-rule strengths in the observed spectrum.

As can be seen from Tables I, IV, and V, there are fragments of the $l = 0$ and $l = 2$ strength between 2.66 and 4.4 MeV, but only the state at 4.32 MeV has appreciable strength. The main interest in the region above 2.66 MeV centers on the observed $l = 1$ and $l = 3$ strengths. In Table V, the listed strengths for these states were normalized by the same factor as that used for the others; i.e., S_{exp} was divided by 2.1 – the normalization factor required to make $(2J+1)S = 4.6$ for the ground state.

It is not yet possible to compare these odd-parity states with any model. Nilsson-model calculations could in principle be performed, but it would be unrealistic to expect large enough shell-model configuration spaces to be available in the near future. However, these results are in qualitative agreement with simple shell-model considerations. The first odd-parity states that should be seen in ^{27}Al$(d, p)^{28}$Al would be

$$[\pi(1d_{5/2})^{-1}\nu(1f_{7/2})]_{1^-,2^-,3^-,4^-,5^-,6^-},$$

followed by

$$[\pi(1d_{5/2})^{-1}\nu(2p_{3/2})]_{1^-,2^-,3^-,4^-}.$$

The sum-rule limit on the $l = 3$ states of the former is $(2J+1)S = 48$, and on the $l = 1$ states of the latter it is $(2J+1)S = 24$. The $l = 1$ and $l = 3$ contributions seen in this experiment represent small fractions (i.e., ~15%) of such limits, and it is not unreasonable to expect that the shell model could allow the lowest fragments of these configurations to appear at 3–4 MeV in ^{28}Al.

VI. CONCLUSION

The reaction ^{27}Al$(d, p)^{28}$Al has been studied at a deuteron energy of 23 MeV. Distorted-wave calculations with several parameter sets indicate that there is difficulty in extracting quantitative spectroscopic information from this direct reaction. Such difficulty may account for some of the discrepancies among various direct-reaction studies in this $A \approx 28$ mass region.

Qualitatively, the results obtained are in reasonable agreement with the shell-model calculation. The states which the model predicted to be strong are observed to be strong, and the states which we observed to be weak are indeed predicted to be weak. However, some states that were observed to be strong were predicted to be weak; these discrepancies may perhaps be indicative of mixings not included in the model. Finally, three odd-parity states are seen at excitation energies below 4.4 MeV.

Note added in proof: After this work was completed, another report of the reaction ^{27}Al$(d, p)^{28}$Al appeared [T. P. G. Carola and J. G. Vander Baan, Nucl. Phys. A173, 414 (1971)]. The results of that study, performed at $E_d = 12$ MeV, are in qualitative agreement with the present results.

---

*Work performed under the auspices of the U. S. Atomic Energy Commission.

† Present address: University of Pittsburgh, Pittsburgh, Pennsylvania.

‡ Present address: University of Pennsylvania, Philadelphia, Pennsylvania.

[1]H. A. Enge, W. W. Buechner, and A. Sperduto, Phys. Rev. 88, 963 (1952); W. W. Buechner, M. Mazari, and A. Sperduto, *ibid.* 101, 188 (1956); E. W. Hamburger, B. L. Cohen, and R. E. Price, *ibid.* 121, 1143 (1961).

[2]H. A. Enge, E. J. Irwin, and D. H. Weaver, Phys. Rev. 115, 949 (1959).

[3]A. H. Wapstra and A. L. Veenendaal, Phys. Rev. 91, 426 (1953); R. K. Sheline, N. R. Johnson, P. R. Bell, R. C. Davis, and F. K. McGowan, *ibid.* 94, 1642 (1954).

[4]B. Zeidman, J. V. Maher, H. T. Fortune, and G. C. Morrison, Bull. Am. Phys. Soc. 14, 1201 (1969).

[5]O. Häuser, T. K. Alexander, D. Pelte, B. W. Hooten, and H. C. Evans, Phys. Rev. Letters 23, 320 (1969); K. Nakai, F. S. Stephens, and R. M. Diamond, Nucl. Phys. A150, 114 (1970); B. H. Wildenthal, J. B. McGrory, and P. W. M. Glaudemans, Phys. Rev. Letters 26, 96 (1971); J. Bar-Touv and I. Kelson, Phys. Rev. 142, 599 (1966).

[6]M. C. Mermaz, C. A. Whitten, Jr., and D. A. Bromley, Phys. Rev. 187, 1466 (1969).

[7]G. Ripka, in *Proceedings of the International Conference on Nuclear Physics, Gatlinburg, Tennessee, 1967,* edited by R. L. Becker (Academic, New York, 1967), p. 833, and references therein.

[8]P. M. Endt and C. Van der Leun, Nucl. Phys. A105, 1 (1967).

[9]J. V. Maher, G. B. Beard, G. Wedberg, E. L. Sprenkel-Segel, A. Yousef, B. H. Wildenthal, and R. E. Segel, following paper, Phys. Rev. C 5, 1322 (1972).

[10]R. J. Ascuito, D. A. Bell, and J. P. Davidson, Phys. Rev. 176, 1323 (1968).

[11]D. O. Boerma and Ph. B. Smith, Phys. Rev. C 4, 1211 (1971).

[12]R. M. Freeman and A. Gallmann, Nucl. Phys. A156,

305 (1970).
[13]B. Zeidman, T. H. Braid, and J. Nolen, to be published.
[14]B. Zeidman, H. T. Fortune, J. V. Maher, and G. C. Morrison, to be published.
[15]J. R. Erskine and R. H. Vonderohe, Nucl. Instr. Methods 81, 221 (1970).
[16]J. R. Comfort, ANL Physics Division Informal Report No. 1970B (unpublished).
[17]J. L. Yntema, private communication.
[18]H. T. Fortune, T. J. Gray, W. Trost, and N. R. Fletcher, Phys. Rev. 179, 1033 (1969).
[19]R. N. Glover and A. D. W. Jones, Nucl. Phys. 81, 268 (1966).
[20]F. G. Perey, Phys. Rev. 131, 745 (1963).
[21]B. A. Watson, P. P. Singh, and R. E. Segel, Phys. Rev. 182, 977 (1969).
[22]G. R. Satchler, Nucl. Phys. A92, 273 (1967).
[23]P. M. Drisko, unpublished.
[24]P. D. Kunz, University of Colorado (unpublished).

PHYSICAL REVIEW C VOLUME 5, NUMBER 4 APRIL 1972

Electromagnetic Transition Rates in ^{28}Al†

J. V. Maher,* G. B. Beard,‡ and G. H. Wedberg§
Argonne National Laboratory, Argonne, Illinois 60439

and

E. Sprenkel-Segel and A. Yousef
Illinois Institute of Technology, Chicago, Illinois 60616, and Argonne National Laboratory, Argonne, Illinois 60439

and

B. H. Wildenthal¶
Michigan State University, East Lansing, Michigan 48823

and

R. E. Segel¶
Northwestern University, Evanston, Illinois 60201, and Argonne National Laboratory, Argonne, Illinois 60439

(Received 15 November 1971)

Lifetimes for the 2nd through 12th excited states in ^{28}Al have been obtained by use of the attenuated-Doppler-shift technique. Combining these results with previous information on this nucleus makes it possible to assign spins to all of the states that have been studied. All of the information is then compared with a shell-model calculation and with other theoretical descriptions that have been advanced.

I. INTRODUCTION

In the simplest shell-model picture, the $1d_{5/2}$ subshell closes at ^{28}Si. While the closeness of the $1d_{5/2}$, $2s_{1/2}$, and $1d_{3/2}$ subshells indicates that this simplest picture can only be a rough approximation to the true situation for the nuclei in the mass-28 region, the level scheme of ^{28}Al does give substantial support to the simple picture. This level scheme is relatively simple for an odd-odd nucleus; it has only seven levels below 2 MeV, and the two lowest states are as predicted by the $(d_{5/2})^{-1}s_{1/2}$ assignment. In order to determine how well a simple picture holds up when the stringent test of predicting electromagnetic transition rates is applied, the present work of measuring the lifetimes of the low-lying states in ^{28}Al was undertaken.

The attenuated-Doppler-shift method was much the same as in earlier Argonne work[1,2]; i.e., the spectra of γ rays in coincidence with each of two proton detectors were recorded. Figure 1 is a schematic diagram of the experimental arrangement. The pulses were processed by conventional electronics, and for each event the proton and γ-ray pulse heights in digitized form were recorded on magnetic tape. The available memory capacity was sufficient for on-line recording of some of the γ-ray spectra of interest, though others had to be obtained by sorting the data stored on the tapes. The Doppler shifts were extracted for those transitions deemed to be most useful in de-